Spherical signal processing for cosmology

Jason McEwen

http://www.jasonmcewen.org/

Department of Physics and Astronomy
University College London (UCL)

17 October 2011 :: UCL, London

Outline

Spherical harmonic transform

- The spherical harmonics are the eigenfunctions of the Laplacian on the sphere: $\Delta_{S^2} Y_{\ell m} = -\ell(\ell+1) Y_{\ell m}$.

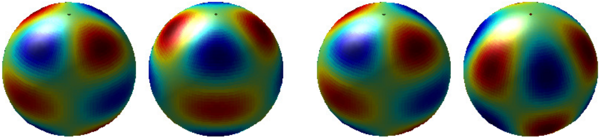

(a) $\ell = 4, m = 2$ (b) $\ell = 4, m = 3$

Figure: Spherical harmonic functions (real and imaginary parts).

- Any square integrable scalar function on the sphere $f \in L^2(S^2)$ may be represented by its spherical harmonic expansion:

$$\boxed{f(\theta, \varphi) = \sum_{\ell=0}^{\infty} \sum_{m=-\ell}^{\ell} f_{\ell m} \, Y_{\ell m}(\theta, \varphi) \, .}$$

- The spherical harmonic coefficients are given by the usual projection onto each basis function:

$$\boxed{f_{\ell m} = \langle f, \, Y_{\ell m} \rangle = \int_{S^2} \mathrm{d}\Omega(\theta, \varphi) \, f(\theta, \varphi) \, Y_{\ell m}^{*}(\theta, \varphi) \, .}$$

- We consider signals on the sphere band-limited at L, that is signals such that $f_{\ell m} = 0, \forall \ell \geq L$.

Spherical harmonic transform

- The spherical harmonics are the eigenfunctions of the Laplacian on the sphere: $\Delta_{\mathrm{S}^2} Y_{\ell m} = -\ell(\ell+1) Y_{\ell m}$.

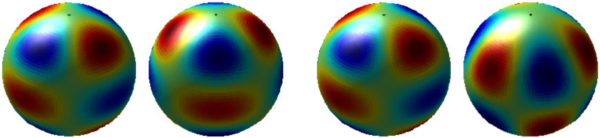

(a) $\ell = 4, m = 2$ (b) $\ell = 4, m = 3$

Figure: Spherical harmonic functions (real and imaginary parts).

- Any square integrable scalar function on the sphere $f \in \mathrm{L}^2(\mathrm{S}^2)$ may be represented by its spherical harmonic expansion:

$$\boxed{f(\theta,\varphi) = \sum_{\ell=0}^{\infty} \sum_{m=-\ell}^{\ell} f_{\ell m}\, Y_{\ell m}(\theta,\varphi)\ .}$$

- The spherical harmonic coefficients are given by the usual projection onto each basis function:

$$\boxed{f_{\ell m} = \langle f,\, Y_{\ell m}\rangle = \int_{\mathrm{S}^2} \mathrm{d}\Omega(\theta,\varphi)\, f(\theta,\varphi)\, Y^{*}_{\ell m}(\theta,\varphi)\ .}$$

- We consider signals on the sphere band-limited at L, that is signals such that $f_{\ell m} = 0,\ \forall \ell \geq L$.

Sampling theorems on the sphere

- Inexact spherical harmonic transforms exist for a variety of pixelisations of the sphere, for example:
    - `HEALpix` (Gorski *et al.* 2005)
    - `IGLOO` (Crittenden & Turok 1998)

  $\rightarrow$ Do **not** lead to sampling theorems on the sphere!

- Sampling theorems state how to represent all information content of a band-limited signal $\rightarrow$ theoretically exact spherical harmonic transforms.

- Driscoll & Healy (1994) sampling theorem:
    - Equiangular pixelisation of the sphere
    - Require $\sim 4L^2$ samples on the sphere
    - Semi-naive algorithm with complexity $\mathcal{O}(L^3)$
      (algorithms with lower scaling exist but they are not generally stable)
    - Require a precomputation or otherwise restricted use of Wigner recursions

A novel sampling theorem on the sphere

- Have developed a new sampling theorem and corresponding fast algorithms by performing a factoring of rotations and then by associating the sphere with the torus through a periodic extension (JDM & Wiaux 2011).
- Similar (in flavour but not detail!) to making a periodic extension in θ of a function ${}_sf$ on the sphere.

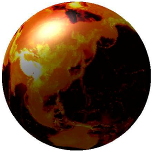

(a) Function on sphere

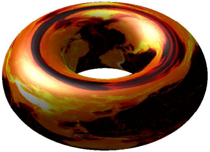

(b) Even function on torus

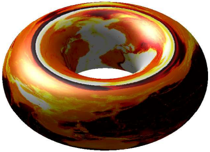

(c) Odd function on torus

Figure: Associating functions on the sphere and torus.

A novel sampling theorem on the sphere

- Properties of our new sampling theorem:
  - Equiangular pixelisation of the sphere
  - Require $\sim 2L^2$ samples on the sphere (and still fewer than Gauss-Legendre sampling)
  - Exploit fast Fourier transforms to yield a fast algorithm with complexity $\mathcal{O}(L^3)$
  - No precomputation and very flexible regarding use of Wigner recursions
  - Extends to spin function on the sphere with no change in complexity or computation time

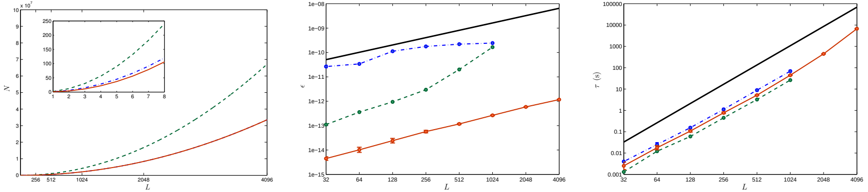

(a) Number of samples (b) Numerical accuracy (c) Computation time

Figure: Performance of our sampling theorem (MW=red; DH=green; GL=blue)

Why wavelets?

Fourier (1807)

Haar (1909)

Morlet and Grossman (1981)

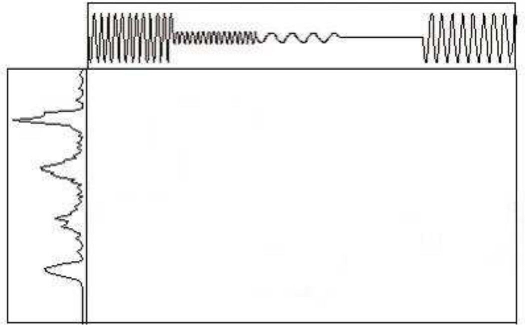

Figure: Fourier vs wavelet transform (image from `http://www.wavelet.org/tutorial/`)

Why wavelets?

Fourier (1807)

Haar (1909)

Morlet and Grossman (1981)

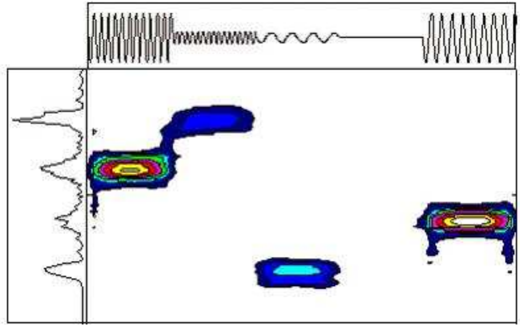

Figure: Fourier vs wavelet transform (image from `http://www.wavelet.org/tutorial/`)

Continuous wavelets on the sphere

- Follow construction derived by Antoine and Vandergheynst (1998) (reintroduced by Wiaux *et al.* (2005)).
- Construct wavelet atoms from affine transformations (dilation, translation) on the sphere of a mother wavelet.
- The natural extension of translations to the sphere are rotations. Characterised by the elements of the rotation group $\mathrm{SO}(3)$, which parameterise in terms of the three Euler angles $\rho = (\alpha, \beta, \gamma)$. Rotation of a function f on the sphere is defined by

$$[\mathcal{R}(\rho)f](\hat{\mathbf{s}}) = f(\rho^{-1}\hat{\mathbf{s}}), \quad \rho \in \mathrm{SO}(3) \ .$$

- How define dilation and admissible wavelets on the sphere?

Stereographic projection

- Apply stereographic projection to build an association with the plane.

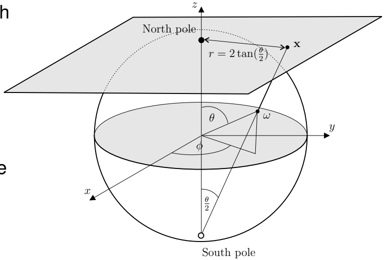

- Stereographic projection operator is defined by $\Pi : \hat{\boldsymbol{s}} \rightarrow \boldsymbol{x} = \Pi\hat{\boldsymbol{s}} = (r(\theta), \varphi)$ where $r = 2\tan(\theta/2)$, $\hat{\boldsymbol{s}} \equiv (\theta, \varphi) \in \mathrm{S}^2$ and $\boldsymbol{x} \in \mathbb{R}^2$ is a point in the plane, denoted here by the polar coordinates (r, φ). The inverse operator is $\Pi^{-1} : \boldsymbol{x} \rightarrow \hat{\boldsymbol{s}} = \Pi^{-1}\boldsymbol{x} = (\theta(r), \varphi)$, where $\theta(r) = 2\tan^{-1}(r/2)$.

- Define the action of the stereographic projection operator on functions on the plane and sphere. Consider the space of square integrable functions in $\mathrm{L}^2(\mathbb{R}^2, \mathrm{d}^2\boldsymbol{x})$ on the plane and $\mathrm{L}^2(\mathrm{S}^2, \mathrm{d}\Omega(\hat{\boldsymbol{s}}))$ on the sphere.
  - The action of the stereographic projection operator $\Pi : f \in \mathrm{L}^2(\mathrm{S}^2, \mathrm{d}\Omega(\hat{\boldsymbol{s}})) \rightarrow p = \Pi f \in \mathrm{L}^2(\mathbb{R}^2, \mathrm{d}^2\boldsymbol{x})$ on functions is defined as

$$p(r, \varphi) = (\Pi f)(r, \varphi) = (1 + r^2/4)^{-1} f(\theta(r), \varphi) \,.$$

  - The inverse stereographic projection operator $\Pi^{-1} : p \in \mathrm{L}^2(\mathbb{R}^2, \mathrm{d}^2\boldsymbol{x}) \rightarrow f = \Pi^{-1} p \in \mathrm{L}^2(\mathrm{S}^2, \mathrm{d}\Omega(\hat{\boldsymbol{s}}))$ on functions is then

$$f(\theta, \varphi) = (\Pi^{-1} p)(\theta, \varphi) = [1 + \tan^2(\theta/2)]\, p(r(\theta), \varphi) \,.$$

Dilation on the sphere

- The spherical dilation operator $\mathcal{D}(a) : f(\hat{\mathbf{s}}) \to [\mathcal{D}(a)f](\hat{\mathbf{s}})$ in $\mathrm{L}^2(\mathrm{S}^2, \, \mathrm{d}\Omega(\hat{\mathbf{s}}))$ is defined as the conjugation by Π of the Euclidean dilation $d(a)$ in $\mathrm{L}^2(\mathbb{R}^2, \, \mathrm{d}^2\boldsymbol{x})$ on tangent plane at north pole:

$$\mathcal{D}(a) \equiv \Pi^{-1} \, d(a) \, \Pi \, .$$

- Spherical dilation given by

$$[\mathcal{D}(a)f](\hat{\mathbf{s}}) = [\lambda(a, \theta, \varphi)]^{1/2} \, f(\hat{\mathbf{s}}_{1/a}) \, ,$$

where $\hat{\mathbf{s}}_a = (\theta_a, \varphi)$ and $\tan(\theta_a/2) = a \tan(\theta/2)$.

- Cocycle of a spherical dilation is defined by

$$\lambda(a, \theta, \varphi) \equiv \frac{4a^2}{[(a^2 - 1)\cos\theta + (a^2 + 1)]^2} \, .$$

Correspondence principle

- Correspondence principle between spherical and Euclidean wavelets states that the inverse stereographic projection of an *admissible* wavelet on the plane yields an *admissible* wavelet on the sphere (proved by Wiaux *et al.* 2005)
- Mother wavelets on sphere constructed from the projection of mother Euclidean wavelets defined on the plane:

$$\Phi = \Pi^{-1}\Phi_{\mathbb{R}^2} \ ,$$

where $\Phi_{\mathbb{R}^2} \in \mathrm{L}^2(\mathbb{R}^2, \, \mathrm{d}^2\boldsymbol{x})$ is an admissible wavelet in the plane.

- Directional wavelets on sphere may be naturally constructed in this setting – they are simply the projection of directional Euclidean planar wavelets on to the sphere.

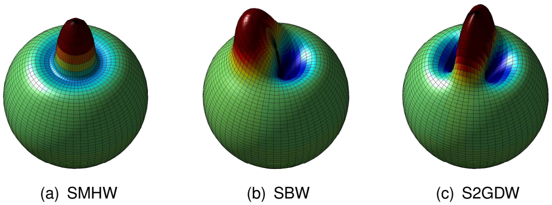

Figure: Spherical wavelets at scale $a, b = 0.2$.

Continuous wavelet analysis formula

- Wavelets on the sphere may now be constructed from rotations and dilations of a mother spherical wavelet $\Phi \in \mathrm{L}^2(\mathrm{S}^2, \, \mathrm{d}\Omega(\hat{\mathbf{s}}))$. The corresponding wavelet family $\{\Phi_{a,\rho} \equiv \mathcal{R}(\rho)\mathcal{D}(a)\Phi : \rho \in \mathrm{SO}(3), \, a \in \mathbb{R}_*^+\}$ provides an over-complete set of functions in $\mathrm{L}^2(\mathrm{S}^2, \, \mathrm{d}\Omega(\hat{\mathbf{s}}))$.
- The CSWT of $f \in \mathrm{L}^2(\mathrm{S}^2, \, \mathrm{d}\Omega(\hat{\mathbf{s}}))$ is given by the projection on to each wavelet atom in the usual manner:

$$\boxed{\widehat{\mathcal{W}}_\Phi^f(a,\rho) = \langle f, \Phi_{a,\rho}\rangle = \int_{\mathrm{S}^2} \mathrm{d}\Omega(\hat{\mathbf{s}}) \, f(\hat{\mathbf{s}}) \, \Phi_{a,\rho}^*(\hat{\mathbf{s}}) \, ,}$$

  where $\mathrm{d}\Omega(\hat{\mathbf{s}}) = \sin\theta \, \mathrm{d}\theta \, \mathrm{d}\varphi$ is the usual invariant measure on the sphere.
- Transform general in the sense that all orientations in the rotation group $\mathrm{SO}(3)$ are considered, thus directional structure is naturally incorporated.
- Fast algorithms essential (for a review see Wiaux, JDM *et al.* 2007)
  - Factoring of rotations: JDM *et al.* 2007
  - Separation of variables: Wiaux *et al.* 2005

Continuous wavelet synthesis formula

- The synthesis of a signal on the sphere from its wavelet coefficients is given by

$$\boxed{f(\hat{s}) = \int_0^{\infty} \frac{\mathrm{d}a}{a^3} \int_{\mathrm{SO}(3)} \mathrm{d}\varrho(\rho) \widehat{\mathcal{W}}_{\Phi}^{f}(a,\rho)\, [\mathcal{R}(\rho)\widehat{L}_{\Phi}\Phi_a](\hat{s}) \ ,}$$

  where $\mathrm{d}\varrho(\rho) = \sin\beta\, \mathrm{d}\alpha\, \mathrm{d}\beta\, \mathrm{d}\gamma$ is the invariant measure on the rotation group $\mathrm{SO}(3)$.

- The $\widehat{L}_{\Phi}$ operator in $\mathrm{L}^2(\mathrm{S}^2,\ \mathrm{d}\Omega(\hat{s}))$ is defined by the action

$$(\widehat{L}_{\Phi} g)_{\ell m} \equiv g_{\ell m}/\widehat{C}_{\Phi}^{\ell}$$

  on the spherical harmonic coefficients of functions $g \in \mathrm{L}^2(\mathrm{S}^2,\ \mathrm{d}\Omega(\hat{s}))$.

- In order to ensure the perfect reconstruction of a signal synthesised from its wavelet coefficients, the admissibility condition

$$\boxed{0 < \widehat{C}_{\Phi}^{\ell} \equiv \frac{8\pi^2}{2\ell+1} \sum_{m=-\ell}^{\ell} \int_0^{\infty} \frac{\mathrm{d}a}{a^3} \mid (\Phi_a)_{\ell m} \mid^2 < \infty}$$

  must be satisfied for all $\ell \in \mathbb{N}$, where $(\Phi_a)_{\ell m}$ are the spherical harmonic coefficients of $\Phi_a(\hat{s})$.

- Exact reconstruction in practice:
  - Multiresolution analysis on the sphere (*e.g.* JDM & Scaife (2008))
  - Steerable scale discretised wavelets (S2DW) (Wiaux, JDM, *et al.* (2008))
  - Spin S2DW for the analysis of polarised signals (JDM, Wiaux, *et al.* (in prep))

Continuous wavelet synthesis formula

- The synthesis of a signal on the sphere from its wavelet coefficients is given by

$$\boxed{f(\hat{\mathbf{s}}) = \int_0^\infty \frac{\mathrm{d}a}{a^3} \int_{\mathrm{SO}(3)} \mathrm{d}\varrho(\rho) \widehat{\mathcal{W}}^f_\Phi(a,\rho)\, [\mathcal{R}(\rho)\widehat{L}_\Phi \Phi_a](\hat{\mathbf{s}})\ ,}$$

  where $\mathrm{d}\varrho(\rho) = \sin\beta\, \mathrm{d}\alpha\, \mathrm{d}\beta\, \mathrm{d}\gamma$ is the invariant measure on the rotation group $\mathrm{SO}(3)$.

- The $\widehat{L}_\Phi$ operator in $\mathrm{L}^2(\mathrm{S}^2, \mathrm{d}\Omega(\hat{\mathbf{s}}))$ is defined by the action

$$(\widehat{L}_\Phi g)_{\ell m} \equiv g_{\ell m} / \widehat{C}^\ell_\Phi$$

  on the spherical harmonic coefficients of functions $g \in \mathrm{L}^2(\mathrm{S}^2, \mathrm{d}\Omega(\hat{\mathbf{s}}))$.

- In order to ensure the perfect reconstruction of a signal synthesised from its wavelet coefficients, the admissibility condition

$$\boxed{0 < \widehat{C}^\ell_\Phi \equiv \frac{8\pi^2}{2\ell+1} \sum_{m=-\ell}^{\ell} \int_0^\infty \frac{\mathrm{d}a}{a^3} \mid (\Phi_a)_{\ell m} \mid^2 < \infty}$$

  must be satisfied for all $\ell \in \mathbb{N}$, where $(\Phi_a)_{\ell m}$ are the spherical harmonic coefficients of $\Phi_a(\hat{\mathbf{s}})$.

- Exact reconstruction in practice:
  - Multiresolution analysis on the sphere (*e.g.* JDM & Scaife (2008))
  - Steerable scale discretised wavelets (S2DW) (Wiaux, JDM, *et al.* (2008))
  - Spin S2DW for the analysis of polarised signals (JDM, Wiaux, *et al.* (in prep))

Compressive sensing on the sphere

- Consider the inverse problem

$$\boxed{\boldsymbol{y} = \Phi \boldsymbol{x} + \boldsymbol{n}\ ,}$$

where:

- the samples of f are denoted by the concatenated vector $\boldsymbol{x} \in \mathbb{R}^N$;
- N is the (possibly incomplete) number of samples on the sphere;
- M noisy measurements $\boldsymbol{y} \in \mathbb{R}^M$ are acquired;
- the measurement operator $\Phi \in \mathbb{R}^{M \times N}$ may represent any linear operator (*e.g.* Fourier measurements, convolution, masking);
- the noise $\boldsymbol{n} \in \mathbb{R}^M$ is assumed to be iid Gaussian with zero mean.

- For example, in radio interferometry the measurement operator $\Phi = \mathbf{M}\,\mathbf{F}\,\mathbf{A}$ incorporates:
  - primary beam $\mathbf{A}$ of the telescope;
  - Fourier transform $\mathbf{F}$;
  - masking $\mathbf{M}$ which encodes the incomplete measurements taken by the interferometer.

Compressive sensing on the sphere

- *Many signals in Nature are sparse*.
- Solve inverse problem by applying a prior on sparsity of the signal in a sparsifying basis Ψ or in the magnitude of its gradient.
- Image is recovered by solving:
  - Basis Pursuit denoising problem

$$\boldsymbol{\alpha}^\star = \underset{\boldsymbol{\alpha}}{\arg\min} \|\alpha\|_1 \ \text{ such that } \ \|\boldsymbol{y} - \Phi\Psi\boldsymbol{\alpha}\|_2 \leq \epsilon \ ,$$

    where the image is synthesising by $\boldsymbol{x}^\star = \Psi\boldsymbol{\alpha}^\star$;
  - Total Variation (TV) denoising problem

$$\boldsymbol{x}^\star = \underset{\boldsymbol{x}}{\arg\min} \|\boldsymbol{x}\|_{\mathrm{TV}} \ \text{ such that } \ \|\boldsymbol{y} - \Phi\boldsymbol{x}\|_2 \leq \epsilon \ .$$

- ℓ_1-norm $\|\cdot\|_1$ is given by the sum of the absolute values of the signal.
- TV norm $\|\cdot\|_{\mathrm{TV}}$ is given by the ℓ_1-norm of the gradient of the signal.
- Define discrete TV norm on the sphere:

$$\int_{\mathrm{S}^2} \mathrm{d}\Omega \, |\nabla f| \simeq \sum_{t=0}^{N_\theta - 1} \sum_{p=0}^{N_\varphi - 1} |\nabla f| \, q(\theta_t) \simeq \sum_{t=0}^{N_\theta - 1} \sum_{p=0}^{N_\varphi - 1} \sqrt{q^2(\theta_t)(\delta_\theta x)^2 + \frac{q^2(\theta_t)}{\sin^2\theta_t}(\delta_\varphi x)^2} = \|x\|_{\mathrm{TV}} \ .$$

- Tolerance ϵ is related to an estimate of the noise variance.

Compressive sensing on the sphere

- *Many signals in Nature are sparse*.
- Solve inverse problem by applying a prior on sparsity of the signal in a sparsifying basis Ψ or in the magnitude of its gradient.
- Image is recovered by solving:
  - Basis Pursuit denoising problem

$$\boldsymbol{\alpha}^\star = \arg\min_{\boldsymbol{\alpha}} \|\alpha\|_1 \text{ such that } \|\boldsymbol{y} - \Phi\Psi\boldsymbol{\alpha}\|_2 \leq \epsilon ,$$

    where the image is synthesising by $\boldsymbol{x}^\star = \Psi\boldsymbol{\alpha}^\star$;
  - Total Variation (TV) denoising problem

$$\boldsymbol{x}^\star = \arg\min_{\boldsymbol{x}} \|\boldsymbol{x}\|_{\mathrm{TV}} \text{ such that } \|\boldsymbol{y} - \Phi\boldsymbol{x}\|_2 \leq \epsilon .$$

- ℓ_1-norm $\|\cdot\|_1$ is given by the sum of the absolute values of the signal.
- TV norm $\|\cdot\|_{\mathrm{TV}}$ is given by the ℓ_1-norm of the gradient of the signal.
- Define discrete TV norm on the sphere:

$$\boxed{\int_{\mathrm{S}^2} \mathrm{d}\Omega\, |\nabla f| \simeq \sum_{t=0}^{N_\theta-1}\sum_{p=0}^{N_\varphi-1} |\nabla f|\, q(\theta_t) \simeq \sum_{t=0}^{N_\theta-1}\sum_{p=0}^{N_\varphi-1} \sqrt{q^2(\theta_t)(\delta_\theta \boldsymbol{x})^2 + \frac{q^2(\theta_t)}{\sin^2\theta_t}(\delta_\varphi \boldsymbol{x})^2} \equiv \|\boldsymbol{x}\|_{\mathrm{TV}} .}$$

- Tolerance ϵ is related to an estimate of the noise variance.

TV inpainting

- Solve toy TV inpainting problem on the sphere to recover full map from incomplete measurements (JDM *et al.* 2011)

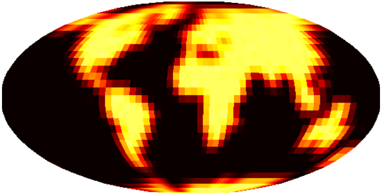

(a) Ground truth

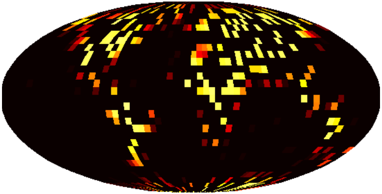

(b) Measurements

Figure: Earth topographic data reconstructed in the harmonic domain for $M/L^2 = 1/2$

TV inpainting

- Solve toy TV inpainting problem on the sphere to recover full map from incomplete measurements (JDM *et al.* 2011)

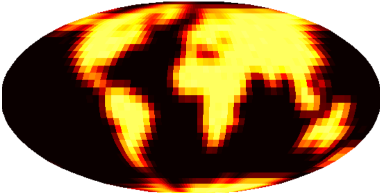

(a) Ground truth

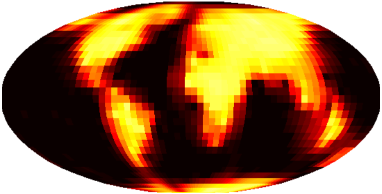

(b) MW reconstruction

Figure: Earth topographic data reconstructed in the harmonic domain for $M/L^2 = 1/2$

Gaussianity of the CMB

- Statistics of primordial fluctuations provide a useful mechanism for distinguishing between various scenarios of the early Universe, such as various models of inflation.
- In the simplest inflationary scenarios, primordial perturbations seed Gaussian temperature fluctuations in the CMB.
- However, this is not the case for alternative inflationary models.
- Evidence of non-Gaussianity in the CMB anisotropies would therefore have profound implications for our understanding of the early Universe.
- Probe WMAP observations of the CMB for evidence of non-Gaussianity.

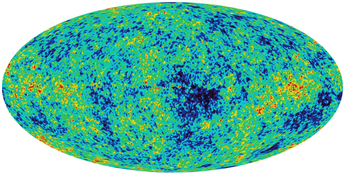

Wavelet analysis of Gaussianity of the CMB

- Various physical processes manifest at different scales and locations
  $\rightarrow$ wavelets ideal tool to probe CMB for deviations from Gaussianity.
- Wavelet coefficients of Gaussian signal remain Gaussian distributed.
- Examine the skewness and kurtosis of wavelet coefficients.
- Compare to Monte Carlo simulations of Gaussian CMB realisations.
- Significant non-Gaussian signal detected in the skewness of wavelet coefficients (JDM *et al*. 2005, 2006, 2008).

Wavelet analysis of Gaussianity of the CMB

- Various physical processes manifest at different scales and locations
  $\rightarrow$ wavelets ideal tool to probe CMB for deviations from Gaussianity.
- Wavelet coefficients of Gaussian signal remain Gaussian distributed.
- Examine the skewness and kurtosis of wavelet coefficients.
- Compare to Monte Carlo simulations of Gaussian CMB realisations.
- Significant non-Gaussian signal detected in the skewness of wavelet coefficients (JDM *et al.* 2005, 2006, 2008).

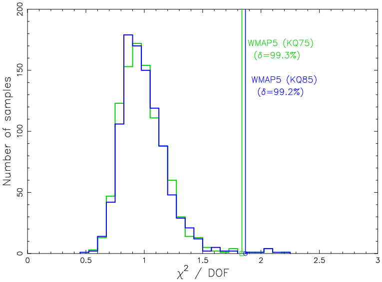

Figure: χ^2 of skewness of wavelet coefficients

Localisation of non-Gaussian features in the CMB

- Localise regions that contribute most significantly to the non-Gaussian signal.
- Detection of the "cold spot" anomaly in the CMB.

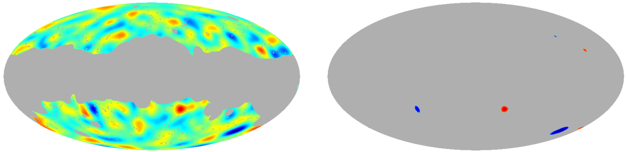

(a) SMHW coefficients

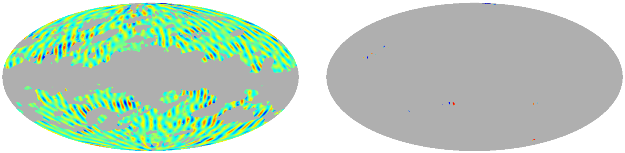

(b) SMW coefficients

Figure: Spherical wavelet coefficient maps (left) and thresholded maps (right)

Dark energy

- Universe consists of ordinary baryonic matter, cold dark matter and dark energy.
- Dark energy represents energy density of empty space. Modelled by a cosmological fluid with negative pressure acting as a repulsive force.
- Evidence for dark energy provided by observations of CMB, supernovae and large scale structure of Universe.

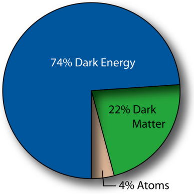

Credit: WMAP Science Team

- However, a consistent model in the framework of particle physics lacking. Indeed, attempts to predict a cosmological constant obtain a value that is too large by a factor of $\sim 10^{120}$.
- Dark energy dominates our Universe but yet we know very little about its nature and origin.
- Verification of dark energy by independent physical methods of considerable interest.
- Independent methods may also prove more sensitive probes of properties of dark energy.

Integrated Sachs-Wolfe (ISW) effect

(ball sim constant movie) (ball sim evolving movie)

Figure: ISW effect analogy

- CMB photons blue (red) shifted when fall into (out of) potential wells.
- Evolution of potential during photon propagation $\rightarrow$ net change in photon energy.
- Gravitation potentials constant w.r.t. conformal time in matter dominated universe.
- Deviation from matter domination due to curvature or dark energy causes potentials to evolve with time $\rightarrow$ secondary anisotropy induced in CMB.

Detecting the ISW effect

- WMAP shown universe is (nearly) flat.
- Detection of ISW effect $\Rightarrow$ direct evidence for dark energy.
- Cannot isolate the ISW signal from CMB anisotropies easily.
- Instead, detect by cross-correlating CMB anisotropies with tracers of large scale structure.
  (Crittenden & Turok 1996)
- Wavelets ideal analysis tool to search for correlation induced by ISW effect since signal manifest at different scales and locations.
  (Pioneered by Vielva *et al.* 2005, followed by JDM *et al.* 2006, JDM *et al.* 2007 and others.)
- Compute correlation of WMAP and NVSS radio galaxy survey and compare to Monte Carlo simulations to determine significance of any candidate detections.

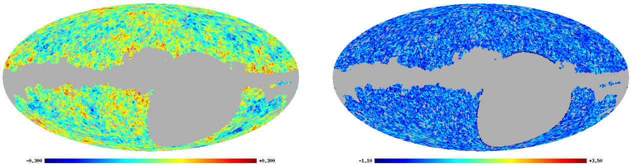

(a) WMAP (b) NVSS

Figure: WMAP and NVSS maps after application of the joint mask

Detection of the ISW effect with wavelets

- Significant correlation detected between the WMAP and NVSS data.
- Foreground contamination and instrumental systematics ruled out as source of the correlation $\Rightarrow$ correlation due to ISW effect.
- Direct observational evidence for dark energy.

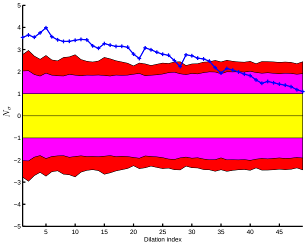

Figure: Wavelet correlation

Constraining dark energy with wavelets

- Possible to use positive detection of the ISW effect to constrain parameters of cosmological models that describe dark energy:
  - Proportional energy density Ω_Λ.
  - Equation of state parameter w relating pressure and density of cosmological fluid that models dark energy, *i.e.* $p = w\rho$.
- Parameter estimates of $\Omega_\Lambda = 0.63^{+0.18}_{-0.17}$ and $w = -0.77^{+0.35}_{-0.36}$ computed from the mean of the marginalised distributions (consistent with other analysis techniques and data sets).

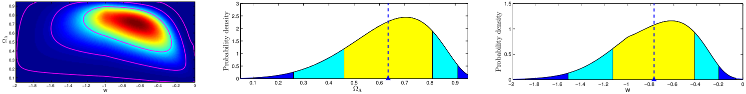

(a) Full likelihood surface
(b) Marginalised distribution for Ω_Λ
(c) Marginalised distribution for w

Figure: Dark energy likelihoods